

## THERMAL GENERATION, DIFFUSION AND DISSIPATION IN 1-3 PIEZOCOMPOSITE SONAR TRANSDUCERS: FINITE ELEMENT ANALYSIS AND EXPERIMENTAL MEASUREMENTS

N. Abboud, J. Mould<sup>†</sup>, G. Wojcik<sup>†</sup>, D. Vaughan<sup>†</sup>, D. Powell<sup>†</sup>, V. Murray<sup>‡</sup>, and C. MacLean<sup>‡</sup>

Weidlinger Associates Inc., 375 Hudson Street, New York, NY 10014, USA

<sup>†</sup>Weidlinger Associates Inc., 4410 El Camino Real, Los Altos, CA 94022, USA

<sup>‡</sup>Fugro-UDI Ltd., Denmore Road, Bridge of Don, Aberdeen, AB23 8JW Scotland, UK

**Abstract** — Thermal management is an important consideration in ultrasound transducer design. It arises in satisfying regulatory and safety requirements in diagnostic and therapeutic ultrasound, as well as in sustaining performance in high power applications such as underwater sonar. A finite element modeling approach was developed to aid in the analysis of this coupled electro-mechanical-thermal problem. The finite element model tracks the damping losses in the electromechanical portion of the problem and converts the lost energy into a thermal dose which constitutes the “input” to the thermal portion of the problem. The resultant temperature spatial and temporal distribution is then solved for. This modeling approach was used to study several 1-3 piezocomposite high power transducers for which experimental data was available. Previous experimental evaluation has demonstrated that these devices can suffer from a degradation in performance due to significant temperature rises at power levels of approximately  $2 \text{ W/cm}^2$  for continuous operation, whereas they can operate efficiently at power levels greater than  $20 \text{ W/cm}^2$  when the duty cycle is reduced below 10%. A detailed thermal analysis of these transducers with respect to efficiency of the thermal dissipation within them is required with a view to understanding and consequently improving the high drive performance of these devices. The goal of this preliminary study is to evaluate the modeling approach and identify key parameters to which the solution is sensitive. Parameters so identified, be they material constants or modeling approaches, will be subject to more complete characterization in follow-up studies aimed at quantitative validation of computational modeling of thermal management in ultrasonic applications.

### INTRODUCTION

Thermal management is an important consideration in ultrasound transducer design. It arises in satisfying regulatory and safety requirements in medical ultrasound, as well as in sustaining performance in high power applications such as in underwater sonar systems. In the medical arena, increasing compactness of upcoming devices limits the usefulness of traditional cures to the thermal problem. In naval applications, new active materials such as PMN and 1-3 composites are being adopted, whether for higher power levels or other performance criteria, and accordingly thermal issues need to be reexamined even in mature applications. The need for a quantitative analysis

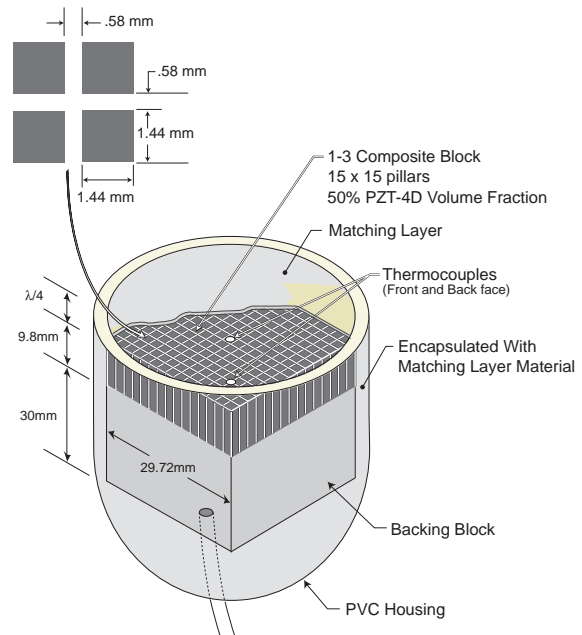


Figure 1 Schematic of 1-3 piezocomposite 150 kHz transducer used for high power evaluation.

tool in such instances is obvious, since experimental prototyping can be costly and does not easily identify specific problem components. In contrast to the spreading acceptance of finite element software for analysis of transducers from an acoustic perspective, no comparable quantitative effort from a coupled thermo-mechanical perspective can be recognized.

In order to address that need, a time-domain finite element modeling approach was developed in PZFlex [1] to aid in the analysis of this coupled electro-mechanical-thermal problem. This approach has already been applied in the context of nonlinear modeling of therapeutic ultrasound, and high intensity ultrasound ablation in particular [2]. In this paper, we focus on its application to device heating rather than tissue heating, and more specifically to the study of several 1-3 piezocomposite high power transducers for which experimental data was available. These transducers were built by Fugro-UDI Ltd. for the purpose of high power evaluation of 1-3 composites, and as such have a relatively simple configuration shown in Fig. 1. The interest in the 1-3 composite material in this case emanates from the flexible nature of this dual phase material which can be utilized to produce large curved, wideband and efficient underwater sonar transducers. The horizontal beamwidth is controlled by the curvature of the composite material. Thus, the cross-sectional area of the active material can be increased to improve the power capability of the device. Although high source levels can be achieved in pulse-mode, the high drive characteristics have not been fully quantified. Experimentation with the "evaluation" transducers has demonstrated that these devices can suffer from a degradation in performance due to significant temperature rises at power levels of approximately 2 W/cm<sup>2</sup> for continuous operation, whereas they can operate efficiently at power levels greater than 20 W/cm<sup>2</sup> when the duty cycle is reduced below 10%. A detailed thermal analysis of these transducers with respect to efficiency of the thermal dissipation within them is required with a view to understanding and consequently improving the high drive performance of these devices.

The goal of this preliminary study is to evaluate the modeling approach and identify key parameters to which the solution is sensitive. Parameters so identified, be they material constants or modeling approaches, will be subject to more complete characterization in follow-up studies aimed at quantitative validation of computational modeling of thermal management in ultrasonic applications.

## COMPUTATIONAL APPROACH

The finite element approach developed in PZFlex tracks the damping losses in the electromechanical portion of the problem and converts the lost energy into a thermal dose which constitutes the "input" to the thermal portion of the problem. The resultant temperature spatial and temporal

distribution is then solved for. The entire cycle of thermal generation, diffusion and dissipation is thus analyzed.

### The Equations of Elasticity and Piezoelectricity

The semidiscrete finite element equations governing elastic (1) and piezoelectric (1)-(2) media are given by:

$$\mathbf{M}_{uu} \frac{d^2 \mathbf{u}}{dt^2} + \mathbf{C}_{uu} \frac{d\mathbf{u}}{dt} + \mathbf{K}_{uu} \mathbf{u} + \mathbf{K}_{u\phi} \Phi = \mathbf{F}_u \quad (1)$$

$$\mathbf{K}_{u\phi}^T \mathbf{u} - \mathbf{K}_{\phi\phi} \Phi = \mathbf{Q} \quad (2)$$

where  $\mathbf{u}$  and  $\Phi$  are the elastic displacement and electric potential solution vectors, respectively,  $\mathbf{F}_u$  and  $\mathbf{Q}$  are the mechanical force and electrical charge vectors, respectively, and  $\mathbf{M}_{uu}$ ,  $\mathbf{C}_{uu}$ ,  $\mathbf{K}_{uu}$ ,  $\mathbf{K}_{\phi\phi}$  and  $\mathbf{K}_{u\phi}$  denote the mass, mechanical damping, elastic stiffness, dielectric stiffness, and piezoelectric coupling matrices, respectively. The solution to these equations is obtained using an explicit-implicit time-stepping scheme [1] and the mechanical damping losses (symbolically  $\mathbf{C}_{uu} d\mathbf{u}/dt$ ) are "tracked" spatially and temporally at each element and assumed fully converted to a heat source for the thermal problem (partial conversion can also be accommodated). Attenuation models and acoustic nonlinearity issues are discussed in detail in [2]

### The Heat Equation

The spatial and temporal distribution of temperature resulting from the conversion of acoustic wave energy into heat is described by the heat equation:

$$\rho c_p \frac{\partial T}{\partial t} = \nabla(\kappa \cdot \nabla T) + f \quad (3)$$

where  $T$ ,  $\rho$ ,  $c_p$ ,  $\kappa$ , and  $f$  are the temperature, density, specific heat or heat capacity, thermal conductivity, and volumetric heat source, respectively.

The discrete finite element form of the heat equation is solved using an implicit time integrator (trapezoidal rule):

$$\left( \frac{2}{\Delta t} \mathbf{M} + \mathbf{K} \right) \mathbf{T}^{n+1} = \mathbf{F}^{n+1} + \mathbf{F}^n + \left( \frac{2}{\Delta t} \mathbf{M} - \mathbf{K} \right) \mathbf{T}^n \quad (4)$$

where  $\mathbf{M}$  and  $\mathbf{K}$  are the capacity and conductivity matrices respectively,  $\mathbf{T}$  is the nodal temperature vector, and superscripts refer to time levels. The thermal load vector  $\mathbf{F}$  corresponds to the lost acoustic energy in the mechanical problem. Equation (4) also allows for the inclusion of a generalized form of the flux boundary condition over the model truncation boundary, based on the static infinite element construct [3], to simulate the temperature diffusion out of the computational domain when the actual medium extends beyond the region modeled.

### Time Scales and Coupling Issues

The basic challenge resides in the efficient yet convenient solution of two mathematical models, namely the elastic wave equation and the heat equation, displaying significantly

different characteristic time scales. In the problem considered below, the 150 kHz transducer vibrates with a period of  $6.7 \times 10^{-6}$  s, and adequate resolution of the waves requires the mechanical solution to advance with time steps no greater than a tenth (and often smaller) of the period. By contrast, the thermal diffusion temporal evolution is adequately resolved with time steps of the order of 0.1 to 1 s. Spatial gradients of the mechanical and thermal fields display a similar scale disparity, permitting coarser discretization for the thermal problem. The solution scheme developed in PZFlex recognizes this disparity and tailors the computational effort expended over each part of the problem to that part's requirements and not to the most stringent requirement of the overall coupled problem. From the perspective of the thermal problem, the ultrasound problem is a steady state event, delivering a constant thermal dose per thermal time step. Thus, analysis of this transient process involves the following steps:

- 1) calculate the ultrasound field over one duty cycle ( or to steady state in CW applications) and calculate the damping losses per cycle (or unit time).
- 2) solve for the resulting transient temperature field.
- 3) if indicated, apply incremental temperature effects to mechanical and thermal material properties and repeat steps 1-3.

If the temperature dependence of material properties is negligible for the heating levels involved, then ultrasound and thermal fields decouple and the calculation stops at 2).

### COMPOSITE TRANSDUCER

The modeling approach described above was applied to the study of a 1-3 composite transducer, with three different matching layer configurations, for which thermal data was already available. These 150kHz transducers, shown in Fig. 1, were built by Fugro UDI Ltd., Aberdeen, Scotland for the purposes of high power evaluation of 1-3 composite based transducers.

The composite block is made of 1.44 x 1.44 x 9.8 mm Morgan Matroc PZT-4D pillars separated by 0.58 mm wide kerf filled with Ciba-Geigy CY1301 polymer. The resulting 15 x 15 pillar block has a 50% ceramic volume fraction, and has one bottom and one top electrode. The backing material is made of highly lossy polyurethane with eccospheres. Three different quarter wavelength matching layers are considered: W.R. Grace STYCAST 2850 KT, W.R. Grace STYCAST 2651 MM, and Emerson & Cuming STYCAST 1264 denoted by ML#1, ML#2 and ML#3 in Table 2, respectively. The matching layers, ML#1 to ML#3, are in order of descending acoustic impedance (from 9.7 MRayls to 3.1 MRayls) and ML#1 is specially engineered for high thermal conductivity. A complete material characterization of PZT-4D was performed by researchers at the Royal Military College of Canada, and results are shown in Table 1. Measured properties for passive materials shown in

Table 2, when available, were provided by the Ultrasonics Group at the University of Strathclyde and Fugro-UDI. Remaining properties, indicated by "~" in Table 2, were estimated on the basis of "typical" values for the general material type. The incomplete knowledge of wavespeeds (particularly the shear components  $v_s$ ), damping and thermal properties should be noted and the "scoping" nature of this preliminary study re-emphasized. In addition, the lack of temperature dependence data for mechanical properties prohibits the analysis of nonlinear effects at this stage (*i.e.* the calculation stops at step 2) in the computational sequence outlined in the section above). Furthermore, the PVC housing was considered to be a perfect thermal insulator and the transducer cable (potentially an important thermal conduction pathway) was not accounted for in the analysis to follow.

| Material Constant                  | PZT-4D Value |
|------------------------------------|--------------|
| $s_{11}^E (m^2/N) \times 10^{-12}$ | 12.00        |
| $s_{12}^E (m^2/N) \times 10^{-12}$ | -3.72        |
| $s_{13}^E (m^2/N) \times 10^{-12}$ | -5.13        |
| $s_{33}^E (m^2/N) \times 10^{-12}$ | 14.94        |
| $s_{44}^E (m^2/N) \times 10^{-12}$ | 32.30        |
| $s_{66}^E (m^2/N) \times 10^{-12}$ | 31.44        |
| $d_{15} (C/N) \times 10^{-12}$     | 369.2        |
| $d_{31} (C/N) \times 10^{-12}$     | -101.1       |
| $d_{33} (C/N) \times 10^{-12}$     | 251.0        |
| $\epsilon_{11}^T / \epsilon_0$     | 1257         |
| $\epsilon_{33}^T / \epsilon_0$     | 1111         |
| $\rho (kg/m^3)$                    | 7568         |
| $Q_m$                              | 600          |
| $cp (J/kg.K)^\S$                   | 420          |
| $\kappa (W/m.K)^\S$                | 1.8          |

Table 1: Measured properties for Morgan Matroc PZT-4D ( $^\S$  Manufacturer's specifications).

| Material Constant          | Filler<br>CY1301 | ML#1<br>2850KT | ML#2<br>2651 | ML#3<br>1264 | Backing<br>Pol/Ecc |
|----------------------------|------------------|----------------|--------------|--------------|--------------------|
| thickness (mm)             | 9.8              | 5.8            | 4.8          | 4.0          | 30.                |
| $v_L (m/s)$                | 2565             | 3508           | 2915         | 2800         | 1250               |
| $v_s (m/s)$                | 1132             | ~1754          | ~1500        | ~1400        | ~625               |
| $\rho (kg/m^3)$            | 1140             | 2768           | 1654         | 1100         | 600                |
| $\alpha_L (dB/m @ 150kHz)$ | 75               | ~75            | ~75          | 81           | 300                |
| $\alpha_s (dB/m @ 150kHz)$ | ~150             | ~150           | ~150         | ~162         | ~600               |
| $cp (J/kg.K)$              | ~1000            | ~1000          | ~1000        | ~1000        | ~1000              |
| $\kappa (W/m.K)^\S$        | 0.22             | 4.20           | 0.60         | 0.22         | ~0.50              |

Table 2: Measured and estimated (~) properties for passive materials used ( $^\S$  Manufacturer's specifications).

The experimental evaluation consisted in driving the submerged transducers with a 10% duty cycle (0.1 ms ON, 0.9 ms OFF) 150 kHz continuous wave for a total duration of 2 minutes, and then measuring the temperature at the composite block backface and frontface thermocouples. Temperature measurements were taken for all three matching layer configurations and at various levels of electrical input power (up to 140, 160 and 300 Watts for ML#1, ML#2, and ML#3 respectively).

### 3D UNIT CELL ANALYSIS

The first model considered consists of a three dimensional unit cell where infinite periodicity of the array in the lateral directions is assumed. The unit cell is defined by a single ceramic pillar surrounded by a half kerf width of CY1301 filler, with a water-loaded matching layer "pad" bonded to the top and a column of polyurethane with ecospheres bonded to the back. This idealization is a sensible first step considering that the thermocouples are located at the center of the composite block, and that the acoustic energy path should be predominantly vertical.

The mechanical portion of the problem is solved for the duration of one duty cycle of 1 ms (0.1 ms ON, 0.9 ms OFF), and the damping energy lost is accumulated. Its distribution is shown in Fig. 2 for the 3 matching layers configurations. Since the distribution of losses is dependent on damping levels as well as on the distribution of acoustic energy, thermal deposition occurs predominantly in the matching layers, and it increases as the impedance matching improves. Since the mechanical properties are currently assumed temperature independent, the rate of thermal deposition remains constant. Furthermore, that rate scales linearly with the input electrical power, and therefore the damping losses per duty cycle and per unit of input electrical power are only calculated once.

The thermal deposition is applied as a source to the thermal problem for a duration of 2 minutes, and the temperature rise is obtained. A comparison of the calculated and measured thermal heating for various input electrical powers and at various locations is shown in Figs. 3 and 4. At the frontface, the calculated temperature is shown at the PZT-4D/matching layer interface and matching layer/water interface, thus providing bounds for thermocouple measurement uncertainties. The correlation is reasonably good at the frontface except at high power levels for ML#3. In the later case, temperature rise up to 30° C are bound to affect the mechanical properties of the polymers: the softening of materials with heating increases damping losses which increases the rate of heating, thus explaining the thermal "runaway" seen in the experimental results. Similarly at the backface, calculated results are shown at the PZT-4D/backing interface as well as 10 mm into the backing away from the interface. The correlation again reasonable, in light of the caveats previously mentioned,

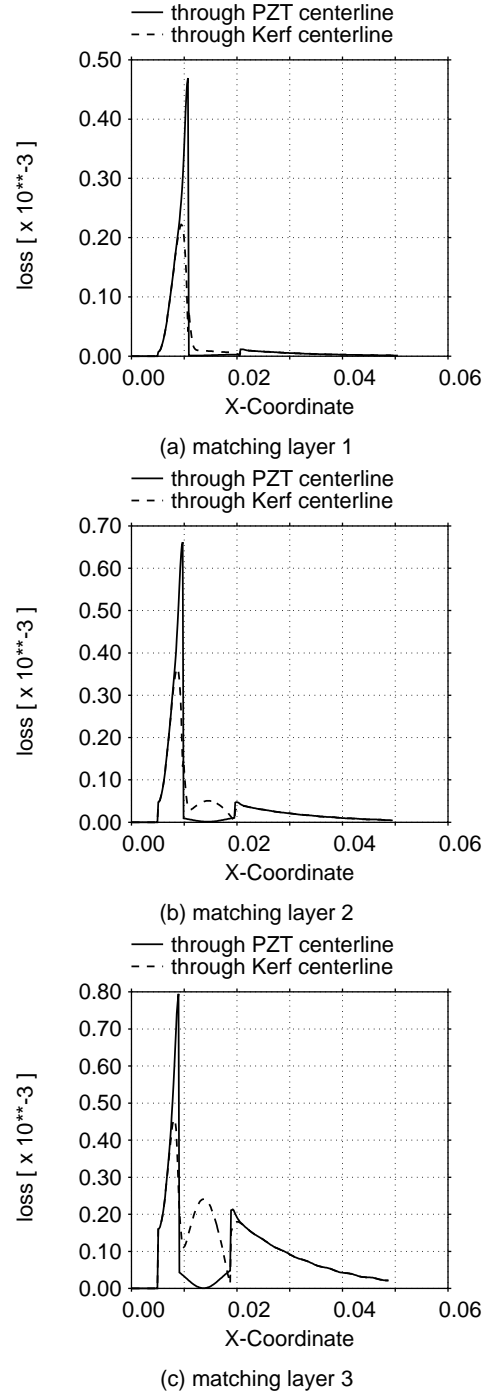


Figure 2 Damping loss or thermal deposition distribution over a 1 ms duty cycle, per volt applied. Distributions along a line, left to right from matching layer to backing block, through the ceramic pillar centerline (solid) and kerf centerline (dashed) are shown.

but the severity of the thermal runaway in the backing of the first configuration (Fig. 4a) is somewhat surprising.

### 2D TRANSDUCER ANALYSIS

The second model considered is a 2D plane strain model of a vertical slice across the transducer, shown in Fig. 5a. This

model was intended to test the hypothesis of a predominantly one-dimensional behavior that motivated the first model. The corresponding distribution of acoustic energy dissipated by damping (Fig. 5b) indicates that lateral standing waves within the composite block create zones of thermal deposition concentration in the filler, backing and matching layer. This would suggest the possibility of occurrence of a lateral distribution of hot spots, clearly not

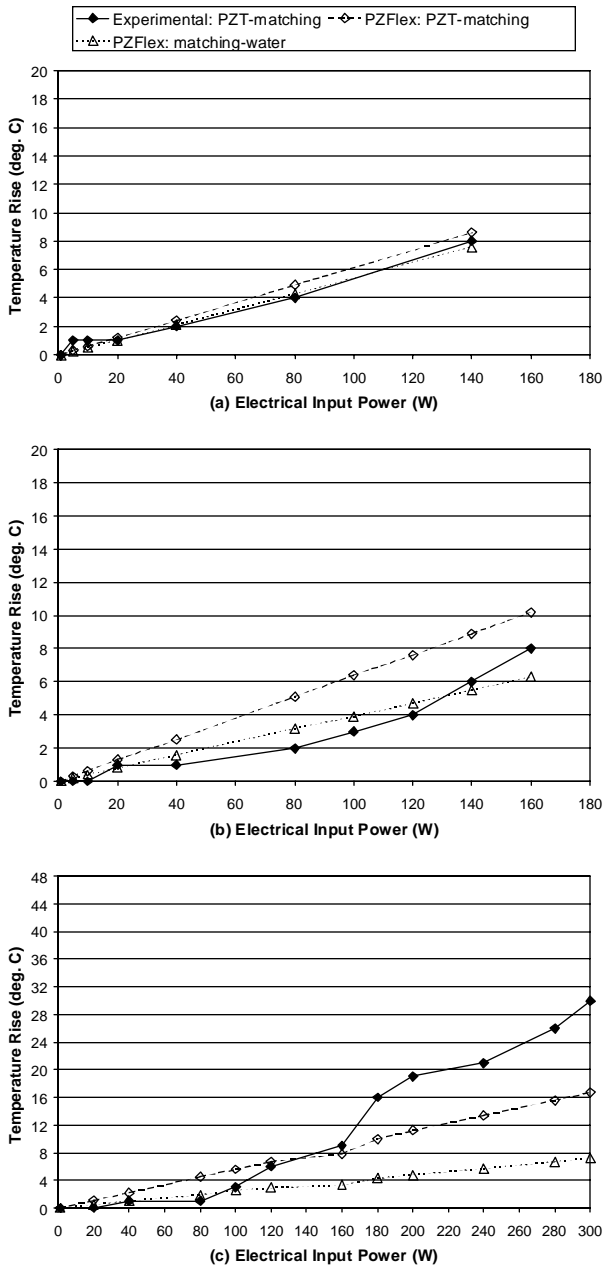


Figure 3 Experimental and calculated frontface temperature rise after 2 min, for Stycast matching layers (a) ML#1 2850KT, (b) ML#2 2651MM, and (c) ML#3 1264.

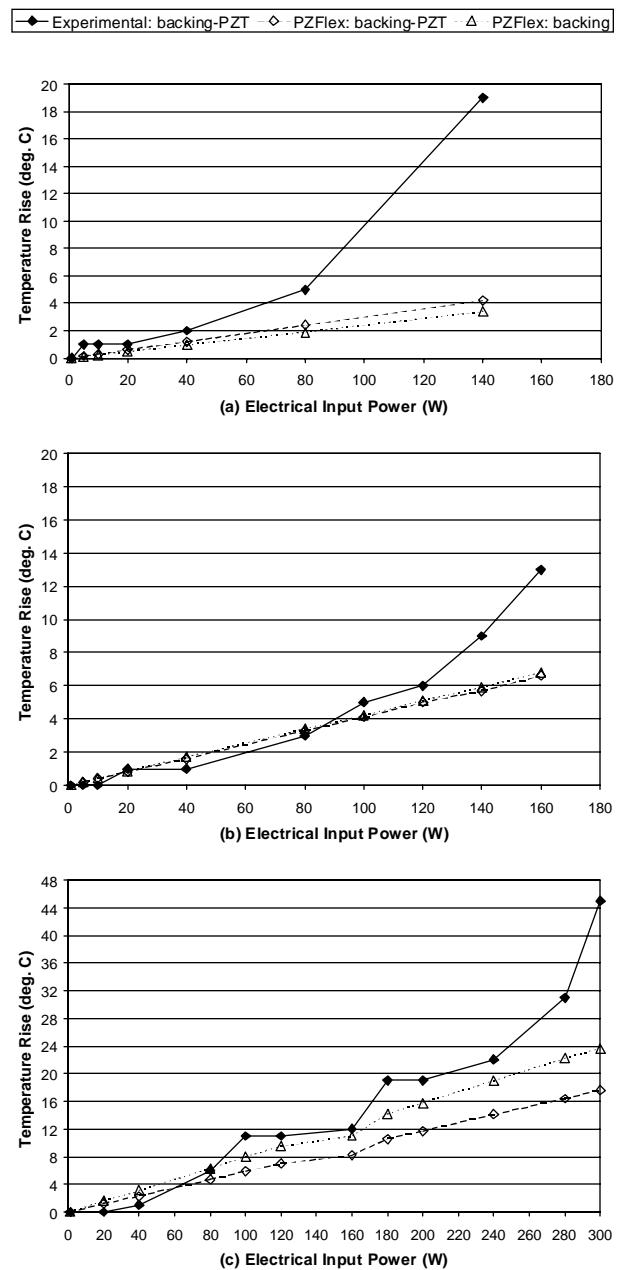


Figure 4 Experimental and calculated backface temperature rise after 2 min, for Stycast matching layers (a) ML#1 2850KT, (b) ML#2 2651MM, and (c) ML#3 1264.

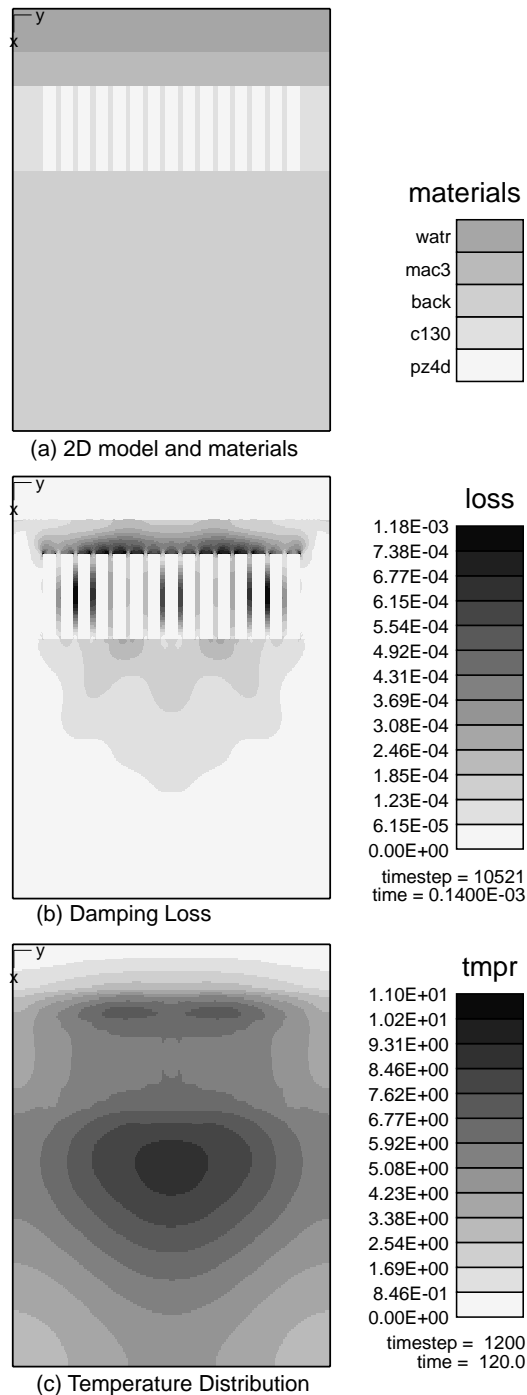


Figure 5 (a) 2D model of transducer with matching layer ML#3 (Stycast 1264), (b) corresponding damping energy lost over a 1 ms 10% duty cycle per volt applied, and (c) resultant temperature rise distribution after 2 min of application of a 150 kHz and 160W input electrical power excitation, in pulse mode.

captured in a 1D model. The thermal diffusion process seems to "smoothen" the field gradients to achieve a less dramatic distribution of temperatures (Fig. 5c), at least at the power level of 160 W considered in this calculation. It is interesting to note though that the maximum temperature does not occur in the center of the matching layer, but rather at a quarter of the lateral dimension. This 2D analysis would indicate that a full 3D model should be considered in future studies, especially at higher power levels where the diffusion process might not be rapid enough to redistribute energy away from hot spots. However, since the 2D temperature levels and their vertical distribution are consistent with the unit cell results, 1D models should remain useful in any initial evaluation.

## CONCLUSIONS

The results of this preliminary study demonstrated the validity and practicality of the coupled electromechanical-thermal finite element scheme developed in PZFlex for simulation of transducer heating. Future work needs to emphasize accurate material characterization if the approach is to be relied upon for its predictive capability in thermal management design for ultrasonic devices. In all cases, characterization of mechanical properties, especially of passive polymers, is crucial to the accurate prediction of acoustic energy distribution [4]. When temperature rises are significant, the thermal dependence of these properties must also be characterized and accounted for.

## ACKNOWLEDGEMENTS

The authors would like to thank G. Hayward and A. Cochran of the University of Strathclyde, Scotland, and S. Sherrit and B. Mukherjee of the Royal Military College of Canada for providing PZT-4D and CY1301 material properties.

## REFERENCES

- [1] G.L. Wojcik, D.K. Vaughan, N.N. Abboud and J. Mould, "Electromechanical modeling using explicit time-domain finite elements," *1993 IEEE Ultrasonics Symp. Proc.*, pp 1107-1112.
- [2] G.L. Wojcik, J. Mould, F. Lizzy, N.N. Abboud M. Ostromogilsky and D.K. Vaughan, "Nonlinear modeling of therapeutic ultrasound," *1995 IEEE Ultrasonics Symp. Proc.*, pp 1617-1622.
- [3] P. Bettess, *Infinite Elements*, Penshaw Press, Cleadon, Sunderland, UK, 1992.
- [4] D.J. Powell *et al.*, "Incremental Model-Build-test validation exercise for a 1D biomedical ultrasonic imaging array," *1997 IEEE Int. Ultrasonics Symp. Proc.*